

# Geometrical decay of the spin Hall effect measured in $\text{Fe}(\text{CsAu})_n$ multilayers

F. Song, H. Beckmann,\* and G. Bergmann

*Department of Physics, University of Southern California, Los Angeles, California 90089-0484, USA*

(Received 1 April 2006; revised manuscript received 3 June 2006; published 26 July 2006)

The Hall effect of  $\text{Fe}(\text{CsAu})_n$  is investigated ( $n$  is an integer). Electrons with spin up and down experience a different degree of specular reflection at the FeCs interface. This yields a different mean free path for the two spin orientations. In the presence of an electric field parallel to the plane of the film one obtains a spin current in addition to the charge current. If one introduces impurities with a large spin-orbit scattering into the Cs host then the combination of spin current and spin-orbit scattering yields a spin Hall effect. By building *in situ* multilayers of CsAu (5 nm of Cs and 0.04 atomic layers of Au) on top of an Fe film one can measure the relative magnitude of the spin current normal to the film. Within the accuracy of the experimental data the spin current in  $\text{Fe}(\text{CsAu})_n$  decays exponentially with a decay length of 20 nm.

DOI: [10.1103/PhysRevB.74.035335](https://doi.org/10.1103/PhysRevB.74.035335)

PACS number(s): 73.50.-h, 72.25.Ba, 73.40.Jn, 73.21.Cd

## I. INTRODUCTION

A conductor with a current  $I_x$  in the  $x$  direction and a magnetic field  $B_z$  in the  $z$  direction experiences an electrical field  $E_y$  in the  $y$  direction perpendicular to the current and magnetic field. This normal Hall effect is due to the orbital motion of the electrons in the presence of a magnetic field. There is another Hall effect which is due to the spin of the electrons. It is, for example, observed in ferromagnetic conductors and generally called anomalous Hall effect (AHE). The AHE was first observed by Hall<sup>1</sup> in the 1880s. It took almost three-quarters of a century before the first quantitative theories were developed.<sup>2,3</sup> The details of the mechanism were very controversial although it was generally accepted that the spin-orbit scattering and the asymmetry between spin-up and spin-down electrons are the essential ingredients for the AHE. Of particular interest was and is the question whether the AHE is due to an asymmetric scattering, known as “skew scattering” or whether the conduction electrons experience a “side jump” in real space. For example, the AHE of single magnetic impurities was derived in the skew scattering model<sup>4</sup> while ferromagnets with a short mean free path are believed to show mainly the side jump.<sup>5</sup> There are still many open questions and a good quantitative theory which covers the whole phenomenon has not yet been developed. Recently an additional mechanism has been under discussion which is connected with the Berry phase and believed to occur even in the absence of any scattering (see, for example, Ref. 6).

Despite the theoretical challenges the AHE has been used in many experiments as a tool. The observation of magnetic dead layers, measurements of the susceptibility of ferromagnets above the Curie temperature, ferromagnetic saturation, moments of magnetic impurities, propagation in real space of conduction electrons, and study of the nature of ferromagnetism in semiconductors are some of the applications.

In addition to the AHE in magnetic materials there is another contribution to the Hall effect in nonmagnetic materials which is due to the spin of the electrons in concurrence with spin-orbit scattering. Hirsch<sup>7</sup> baptized this effect the “spin Hall effect.” An impurity with a strong spin-orbit interaction scatters spin-up electrons with left-right asymmetry. Spin-

down electrons experience the opposite asymmetry. A current through a thin film with strong spin-orbit scatterers yields an accumulation of spin-up electrons on the left rim and spin-down electrons on the right rim of the film (or vice versa). This yields a gradient of the chemical potential perpendicular to the current. The sign of the gradient is opposite for spin-up and spin-down electrons and no electric field is observed as long as density, mean free path, etc. of spin-up and spin-down electrons are identical.

This asymmetric scattering of conduction electrons by spin-orbit scatterers was already investigated by Ballentine and Huberman<sup>8,9</sup> almost 30 years ago. They explained the deviations of the Hall constant from the free electron values for heavy liquid metals such as Tl, Pb, and Bi. They calculated the spin-orbit scattering using perturbation theory. Recently one of the authors<sup>10</sup> calculated exactly the AHE of a polarized electron gas in the presence of spin-orbit scattering (SOS) in terms of Friedel phase shifts.

The opposite left-right asymmetry of spin-up and spin-down scattering by spin-orbit interaction yields two related effects in zero magnetic field.

(1) For a pure charge current the spin-up and spin-down electrons are scattered to opposite sides of the original trajectory. The SOS does not generate a charge imbalance. However, it creates opposite gradients in the chemical potential for spin-up and spin-down electrons. This effect has been predicted by Dyakonov and Perel<sup>11</sup> and Hirsch.<sup>7</sup> (For the more recent theoretical development see, for example, Ref. 12 and references therein.) The spin Hall effect has been recently observed in semiconducting samples.<sup>13,14</sup>

(2) In a spin current spin-up and spin-down electrons have opposite (drift) velocity. Therefore a spin-orbit scatterer deflects both spins to the same side. This generates a transverse electric field.

Both phenomena are two sides of the same effect. We will use the notation as introduced by Hirsch and call this effect “spin Hall effect.” In this paper we will use the following notation. Whenever we subtract the normal Hall resistance from the experimentally measured total Hall resistance we denote the difference as the anomalous Hall resistance. We consider the spin Hall effect and the Hall effect of magnetic material as subgroups of the AHE. If we want to distinguish

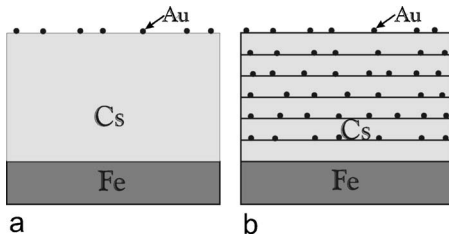


FIG. 1. (a) A single Au coverage of an FeCs double layer. (b) The geometry of  $\text{Fe}(\text{CsAu})_\nu$  multilayers. The thickness of the Fe film is  $d_{\text{Fe}}=9.0$  nm, the repeated multilayers of CsAu have  $d_{\text{Cs}}=5$  nm and a Au coverage of 0.04 atomic layer.

the two subgroups we refer to them as spin AHE and magnetic AHE.

The investigation of spin currents, the anomalous Hall effect, and particularly the spin Hall effect have been attracting considerable interest in the past decades. The possible applications in spintronics<sup>15–18</sup> will further accelerate the exploration of this interesting field.

In this paper we investigate spin currents with the help of spin-orbit scattering impurities. Recently our group investigated the anomalous Hall effect in double layers of FeCs which were covered with submonolayers of Pb and Au.<sup>19</sup> When a double layer of FeCs with  $d_{\text{Fe}}=12.4$  nm and  $d_{\text{Cs}}=29.6$  nm was covered with 1/50 of a monolayer of Pb it showed a remarkable result. The AHE increased by about a factor of 5 when the FeCs double layer was covered with 1/50 of a monolayer of Pb. [The geometry of the layers is shown in Fig. 1(a).] In this spatial configuration the contribution of a Pb atom to the AHE was stronger by a factor of  $2 \times 10^4$  than that of an Fe atom. If the FeCs double layer was covered with 1/50 of an atomic layer of Au then the AHE had the opposite sign and was about a factor of 4 smaller.

Since Pb and Au are nonmagnetic they do not yield a magnetic AHE. Instead the AHE has to be due to a spin current in the Cs. The origin of the spin current is due to the fact that spin-up and spin-down electrons experience a different exchange potential on the Fe side of the FeCs interface. This yields a different specular reflection of spin-up and spin-down electrons at the interface. As a consequence spin-up and spin-down electrons have different mean free paths (MFP) and, in the presence of an electric field, different drift velocities. [The large MFP in the Cs and the high degree of specular reflection at the upper surface (of the order of 80–90%) enhanced this effect.] The spin current is the difference between the spin-up and spin-down currents. Since the host Cs is nonmagnetic the carrier concentration of spin-up and spin-down electrons is equal to half the electron density  $n/2$  and the spin current is equal to  $j_s = n(-e)(v_+ - v_-)/2$ . Our observation of the AHE in FeCsPb layers was an early observation of the spin Hall effect. The mechanism will be discussed in more detail in the Discussion and the Appendix.

The goal of this paper is to investigate the development of the spin current as a function of film thickness. We prepare multilayers consisting of an Fe film which is covered in several steps with sequences of 5 nm of Cs and an impurity coverage of 0.04 atomic layer of a noble metal [see Fig.

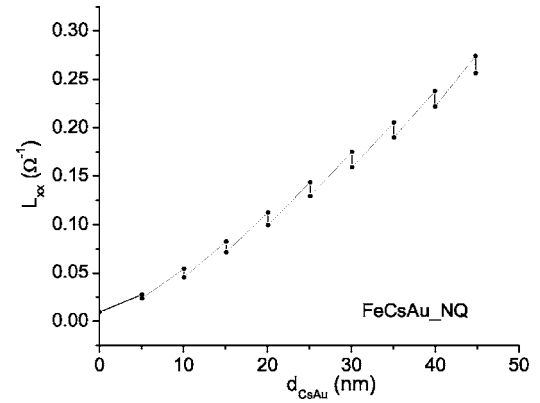


FIG. 2. The experimental conductance  $L_{xx}$  of the  $\text{Fe}(\text{CsAu})_\nu$  multilayer for successive condensation of the Cs and Au layers. The abscissa is the total thickness of the  $(\text{CsAu})_\nu$  multilayers.

1(b)]. For the noble metal we use (i) the strong spin-orbit scatterer Au and (ii) the weak spin-orbit scatterer Ag. The Au and Ag impurities differ strongly in their spin-orbit scattering but are otherwise very similar.

In this paper we use the following abbreviations: AHE = anomalous Hall effect, AHC = anomalous Hall conductance, AH... = anomalous Hall..., MFP = mean free path, and SOS = spin-orbit scattering.

## II. EXPERIMENT

The preparation of the multilayers and the measurements are performed *in situ* in an evaporation cryostat. During the whole experiment the evaporation cryostat is inserted into the liquid helium bath of a superconducting magnet. All the walls surrounding the sample are at liquid helium temperature, while the walls surrounding the evaporation sources are at liquid  $\text{N}_2$  temperature. The vacuum in our system is better than  $10^{-11}$  Torr.

A thin Fe film with a thickness of about 10 nm and a resistance of about  $100 \Omega$  is quench condensed onto a 4.5 K cold quartz substrate. The Fe film is annealed to 40 K. Then the Fe film is covered with a Cs film of 5 nm and annealed to 12 K. In the next step 0.04 atomic layer of Au is evaporated on top of the Cs film, acting as Au impurities. Again the sandwich is annealed to 12 K. This CsAu evaporation sequence is repeated several times. The Cs is evaporated from a SAES-Getters evaporation source. The evaporation rates of the Cs and Au sources are calibrated before and after the evaporation. After each Au evaporation, we have an  $\text{Fe}(\text{CsAu})_\nu$  sandwich (where  $\nu$  can be 1, 2, 3, ...).

After each evaporation (and annealing) the magnetoresistance and the Hall resistance of the sample are measured. The measurements are conducted in the external magnetic field range between  $-7$  and  $+7$  T and at the temperature of 8 K. An identical procedure is used to prepare and investigate  $\text{Fe}(\text{CsAg})_\nu$  multilayers.

In Fig. 2 the conductance  $L_{xx}$  of an  $\text{Fe}(\text{CsAu})_\nu$  multilayer is plotted as a function of the Cs(Au) thickness  $d_{\text{Cs}}$ . Each time the Cs surface is covered with 0.04 atomic layer of the noble metal the conductance is reduced.

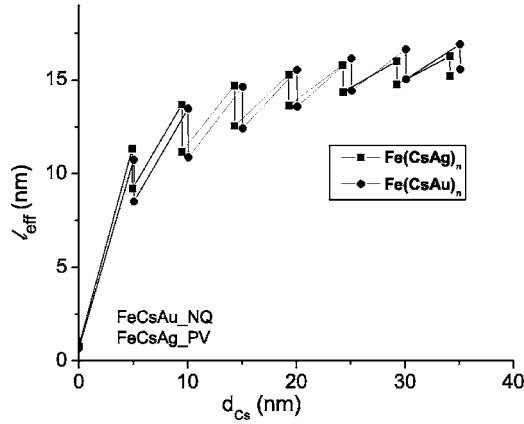


FIG. 3. The experimental effective mean free path of the  $(\text{CsAg})_\nu$  and  $(\text{CsAu})_\nu$  multilayers as a function of the total Cs film thickness, including the Ag or Au impurities.

In the following we want to compare the AHE between the  $\text{Fe}(\text{CsAu})_\nu$  and the  $\text{Fe}(\text{CsAg})_\nu$  multilayers. Therefore it is important that the two impurities, Au and Ag, have essentially the same scattering cross section for the host Cs. Besides the large difference in the spin-orbit scattering Au and Ag are very similar. Both introduce one valence electron and they have an almost identical atomic volume of  $17 \times 10^{-30} \text{ m}^3$ . We calculated the effective conductivity of the Cs film  $\sigma_{xx} = [L_{xx}(d_{flm}) - L_{xx}(d_{\text{Fe}})] / (d_{flm} - d_{\text{Fe}})$ . Here  $d_{flm} = d_{\text{Fe}} + d_{\text{Cs}}$  is the total film thickness. Using the free electron model  $\sigma_{xx}$  yields the effective MFP  $l_{eff}$  of the conduction electrons in the Cs with Au impurities. The same calculation is performed for the  $\text{Fe}(\text{CsAg})_\nu$  multilayers. In Fig. 3, the effective mean free paths  $l_{eff}$  of the conduction electrons in the Cs are plotted for  $(\text{CsAu})_\nu$  and  $(\text{CsAg})_\nu$  multilayers as a function of the total Cs thickness  $d_{\text{Cs}}$ . The similarity between the  $\text{Fe}(\text{CsAu})_\nu$  and the  $\text{Fe}(\text{CsAg})_\nu$  multilayers is quite striking. The first 5 nm thick Cs film has an  $l_{eff}$  of about 12 nm. Then the coverage with 0.04 atomic layer of Au or Ag reduces  $l_{eff}$  by about 4 nm. The data show that  $l_{eff}$  increases with increasing total Cs thickness approaching a value of about 17 nm.

The measurement of the Hall resistance yields the AH conductance. In Fig. 4 the anomalous Hall conductance is plotted as a function of the applied magnetic field for the multilayers  $\text{Fe}(\text{CsAu})_\nu$ , where  $1 \leq \nu \leq 7$ . The normal Hall conductance is subtracted and the antisymmetric part  $[L_{xy}(+B) - L_{xy}(-B)]/2$  is plotted. The AHC is constant at large fields and can be extrapolated to  $B=0$  (as shown in the upper curve). This yields the AHC  $L_{xy,0}$  in zero magnetic field.

In Fig. 5 the zero field AHC  $L_{xy}^0$  is plotted versus the thickness of the multilayers of  $(\text{CsAu})_\nu$  and  $(\text{CsAg})_\nu$  (the Fe thickness subtracted). Obviously the two systems behave very differently.

### III. DISCUSSION

#### A. The $\text{Fe}(\text{CsAg})_\nu$ multilayers

The pure but very disordered Fe film has an AH conductance of about  $1.5 \times 10^{-5} \Omega^{-1}$ . When the first Cs film is su-

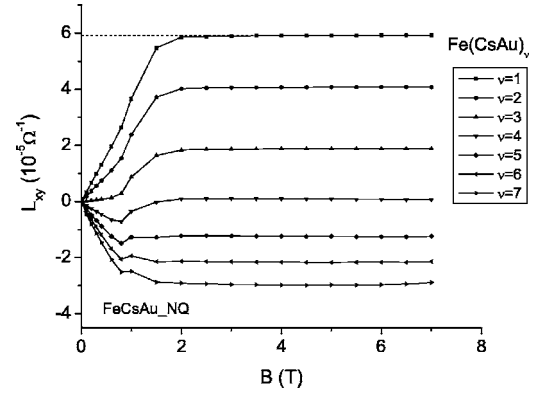


FIG. 4. The experimental anomalous Hall conductance of an  $\text{Fe}(\text{CsAu})_\nu$  multilayer as a function of the applied magnetic field for different numbers of layers  $\nu$ .

perimposed the AH conductance increases to a value of about  $5.5 \times 10^{-5} \Omega^{-1}$  as shown in Fig. 5. This “induced” AHE is a well-known phenomenon which has been analyzed by one of the authors<sup>20,21</sup> in a simple model. Its origin is briefly recalled in the Appendix. The origin of the AH conductance in the  $\text{Fe}(\text{CsAg})_\nu$  multilayer is purely of magnetic origin.

#### B. The $\text{Fe}(\text{CsAu})_\nu$ multilayers

Since the mean free path in  $\text{Fe}(\text{CsAu})_\nu$  is essentially identical to that in the  $\text{Fe}(\text{CsAg})_\nu$  multilayers it experiences the same magnetic AH conductance as the  $\text{Fe}(\text{CsAg})_\nu$  multilayers. But there is obviously an additional effect as Fig. 5 demonstrates. In this paper we will focus on the additional effect, i.e., the difference between the two multilayers.

The AHC drops clearly when the first 0.04 atomic layer of Au is condensed onto the Cs. The difference between the CsAu and the CsAg has to be due to the spin-orbit scattering of the Au. It indicates that there is a spin current in the Cs layer.

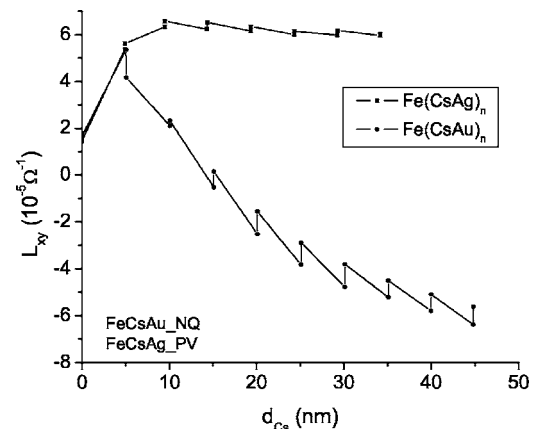


FIG. 5. The extrapolated anomalous Hall conductance for an  $\text{Fe}(\text{CsAg})_\nu$  and the  $\text{Fe}(\text{CsAu})_\nu$  multilayer for successive condensation of the Cs and noble metal layers. The abscissa is the total Cs thickness  $d_{\text{Cs}}$  in the multilayers.

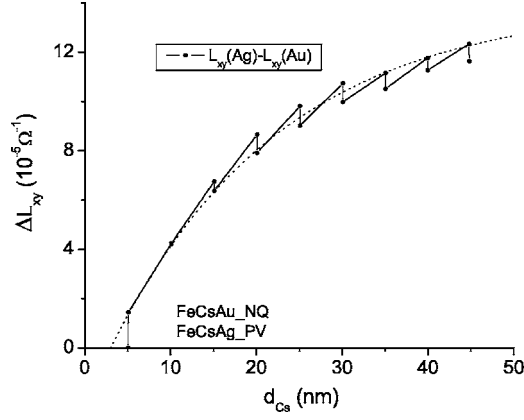


FIG. 6. The (negative) spin Hall effect in  $\text{Fe}(\text{CsAu})_\nu$  multilayer. It is the difference in the AHC between the  $\text{Fe}(\text{CsAg})_\nu$  and the  $\text{Fe}(\text{CsAu})_\nu$  multilayers. The full points are experimental results. The dotted curve represents an exponential fit with  $\Delta L_{xy} = 1.4 \times 10^{-4} \times \{1 - \exp[-(d_{\text{CsAu}} - 3 \text{ nm})/20 \text{ nm}]\} \Omega^{-1}$ .

To simplify the discussion we have plotted in Fig. 6 the difference in the AHC between the  $\text{Fe}(\text{CsAg})_\nu$  and the  $\text{Fe}(\text{CsAu})_\nu$  multilayers. It is important to remember that the additional contribution of the  $\text{Fe}(\text{CsAu})_\nu$  is negative and Fig. 6 shows the absolute value of the difference. This AHC  $\Delta L_{xy}^0$  is caused by the spin-orbit scattering of the Au. Again this proves that we have a spin current in the Cs film. The Au atoms measure the local spin current density, and  $\Delta L_{xy}^0$  is proportional to the integrated spin current density.

First we discuss the results for the multilayers with an equal number  $\nu$  of Cs and Au coverages  $(\text{CsAu})_\nu$ . The magnitude of  $\Delta L_{xy}^0$  increases with  $\nu$  and levels off for larger thicknesses of the  $(\text{CsAu})_\nu$ . This means that the spin current extends quite deep into the  $(\text{CsAu})_\nu$  multilayer. We expect that the electrons in the  $(\text{CsAu})_\nu$  are essentially unpolarized except very close to the FeCs interface. Therefore the spin current is solely caused by the different drift velocities of the spin-up and spin-down electrons. As a consequence any scattering process that destroys the drift velocity will also destroy the spin current. Therefore we expect that the spin current decays exponentially with the distance from the interface as  $J_s^0 \exp(-z/l_{chr})$  and the decay length  $l_{chr}$  is of the order of the MFP. If the Au atoms would be homogeneously distributed in the Cs then the AH conductance would integrate the spin Hall effect over the film thickness. This yields for  $\Delta L_{xy}$

$$\Delta L_{xy} \propto \int_0^d \exp(-z/l_{chr}) dz \propto \left[ 1 - \exp\left(-\frac{d}{l_{chr}}\right) \right].$$

In reality the Au impurities are located at discrete distances of  $\nu d_{\text{Cs}}$  ( $\nu=1, 2, \dots$ ) from the FeCs interface. This modifies the result for  $\Delta L_{xy}$  slightly. We find a good fit of the experimental data with the function  $\Delta L_{xy} = 1.4 \times 10^{-4} \times \{1 - \exp[-(d_{\text{CsAu}} - 3 \text{ nm})/20 \text{ nm}]\} \Omega^{-1}$ . This function is plotted in Fig. 6 as a dashed curve. The experimental characteristic length is  $l_{chr} = 20 \text{ nm}$ . In the Appendix we derive the spatial dependence of the spin current.

### 1. The Au-surface effect

Next we discuss the effect of the Cs and Au evaporation in more detail. Only for  $\nu=1$  does the Au condensation yield an increase of the AHC. For  $\nu=2$  the effect of the Au condensation is very small and for larger  $\nu$  the AHC actually decreases. From Fig. 2 one recognizes that the condensation of Au onto the Cs reduces the conductance of the multilayer. This reduction is equivalent to the conductance of about 2 to 2.5 nm of Cs.

This agrees well with a rather surprising observation that we made in a previous investigation. There we condensed Pb and Au onto an FeCs double layer. The Pb and Au introduced an additional AHC, but the dependence of the  $\Delta L_{xy}$  on the coverage of the surface impurities was quite unexpected. For a coverage of  $d_{\text{pb}}$  or  $d_{\text{Au}}$  of about 0.03 atomic layer  $\Delta L_{xy}$  showed a large extremum, and at a coverage of 0.2 atomic layer  $\Delta L_{xy}$  had almost completely disappeared. Our interpretation of this behavior was that impurities at the surface introduced so much disorder close to the surface that (i) most of the spin current decayed before it reached the Pb (Au) impurities at the surface and (ii) the spin-orbit scattered electrons could not generate much current in the  $y$  direction because their MFP was so short. Our experimental data in Fig. 5 or Fig. 6 demonstrate that this reduction of the MFP is so dominant that after each Au evaporation  $\Delta L_{xy}$  reduces. The new Au impurities do not generate any significant additional AHC, and the AHC of the lower Au layer is reduced because of the MFP reduction.

This reduction of the MFP in the last Cs layer can be (i) a reduction in the whole last Cs layer by a factor of 2 or (ii) a reduction to zero in the upper 2 nm of Cs. The latter case corresponds to electron localization at the upper surface due to the impurities. In the Appendix we will give some arguments for the latter case.

## IV. CONCLUSION

The anomalous Hall effect in  $\text{Fe}(\text{CsAu})_\nu$  multilayers has been investigated. It is compared with the AHE of  $\text{Fe}(\text{CsAg})_\nu$  multilayers. Although the two kinds of impurities cause almost identical normal scattering and the MFPs in the resulting multilayers are essentially the same, the AHE is quite different. The function of the Fe layer is to provide a spin dependent potential at the interface. This yields a different specular reflection of spin-up and spin-down electrons at the FeCs interface. The role of the magnetic field is to align the Fe magnetization perpendicular to film surface. All Hall resistances are back-extrapolated to zero magnetic field. Therefore the reported results represent zero magnetic field results. The different specular reflection of spin-up and spin-down electrons at the FeCs interface represents a source of spin current. The difference in the AH conductance  $\Delta L_{xy}$  of  $\text{Fe}(\text{CsAu})_\nu$  and  $\text{Fe}(\text{CsAg})_\nu$  multilayers is due to the spin current which experiences the spin-orbit scattering of the Au impurities. This effect has been baptized “spin Hall effect.”

By condensing a series of CsAu layers the size of the spin current can be analyzed geometrically. It decays as  $[1 - \exp(-z/l_{chr})]$  where  $z$  is the distance from the interface

and  $l_{chr}$  is a length which has a value of  $l_{chr}=20$  nm.

During the preparation of the multilayers a thin 0.04 atomic layer thick Au layer is condensed onto a fresh 5 nm thick Cs layer. Each time the longitudinal conductance  $L_{xx}$  is reduced by  $\Delta L_{xx}$ . This  $\Delta L_{xx}$  corresponds to the conductance of about 2 nm of Cs. It is suggested that this is a (precursor of) surface localization of the conduction electrons in the Cs. Such an effect has recently been observed in the superconducting proximity effect of PbK double layers.<sup>22</sup>

### ACKNOWLEDGMENT

This research was supported by the National Science Foundation NIRT program, DMR-0439810.

### APPENDIX

#### 1. Origin of the induced anomalous Hall effect

The pure but very disordered Fe film in the  $\text{Fe}(\text{CsAg})_v$  multilayer has an AH conductance of about  $1.5 \times 10^{-5} \Omega^{-1}$ . When Fe is covered with the CsAg film the AH conductance increases with the coverage (as is shown in Fig. 5). This is due to the following facts.<sup>20,21</sup>

(i) If the electric field in the Fe points in the  $x$  direction then the current has a finite  $y$  component [which represents the AH conductance of the Fe film  $L_{yx}(\text{Fe})=d_{\text{Fe}} \times j_y/E_x$ ]. A fraction of the conduction electrons cross the interface into the Cs and carry with them their  $y$  component of the current. This current in  $y$  direction yields an additional contribution, the Hall conductance  $L_{xy}$ . This induced AH conductance increases with the Cs thickness. It saturates when the Cs thickness reaches about half the mean free path in the Cs.

(ii) The second contribution is caused by the electrons which are accelerated in the Cs. When those electrons cross into the Fe they have a much larger drift velocity than the native Fe electrons. They therefore yield a strongly enhanced AH conductance within a thin layer of the Fe. This layer has a thickness of about half the mean free path of the Fe electrons.

Both contributions are of the same order of magnitude and contribute to the increase in the AH conductance of the  $\text{Fe}(\text{CsAg})_v$  multilayer. The role of the Ag impurities lies in the limitation of the mean free path to about 17 nm. Therefore the increase of the AH conductance levels out at about 10 nm. This mechanism of the induced AHE depends on the AHE in the Fe layer and the mean free paths in the Fe and the Cs.

#### 2. Origin of the spin current

We can imagine two different origins of the spin current in the Cs film, (i) transfer of the spin current in the ferromagnetic Fe film through the FeCs interface and (ii) different specular reflection of the spin-up and spin-down electrons in the Cs at the FeCs interface. The experimental data favor the second mechanism as the following discussion shows.

(i) The spin-up and spin-down electrons in the Fe have different densities and MFPs. Therefore the spin-up and spin-down current densities in the Fe are different. This represents

a spin current which could cross the FeCs interface and enter the Cs film. The resulting spin current density  $j_s$  at the upper Cs surface should be at best independent of the Cs thickness. Any scattering within the Cs should reduce  $j_s$  at the free Cs surface. Experimentally we observe, however, a larger AH conductance for the first Au coverage when the Cs thickness is larger. In a previous experiment we covered an FeCs double layer ( $d_{\text{Cs}}=27.5$  nm) with 0.02 atomic layer of Au and observed  $\Delta L_{xy}=-8.8 \times 10^{-5} \Omega^{-1}$ . In the present experiment we covered the FeCs double layer ( $d_{\text{Cs}}=5$  nm) with 0.04 atomic layer of Au and observed  $\Delta L_{xy}=1.2 \times 10^{-5} \Omega^{-1}$ . Although the Au coverages are not identical it is obvious that the larger Cs thickness yields a larger spin current density at the free surface.

(ii) The spin-up and spin-down electrons in the Cs experience a different degree of specular reflection at the FeCs interface. These electrons have accumulated a finite drift velocity before they are reflected. This drift velocity increases with larger Cs thickness because the effective MFP increases. The resulting spin current after the reflection is proportional to the current before the reflection. Therefore the spin current density at the free surface increases with increasing Cs thickness. This is the experimental observation.

### 3. Theoretical description of the spin current

#### a. Homogeneous spin current

Let us first consider a spin current in a nonmagnetic metal film with a constant spin current density  $j_s$ . The metal contains normal and spin-orbit scattering impurities. The total relaxation time  $\tau_0$  is the same for spin-up and spin-down electrons. In addition the SOS impurities scatter spin-up and spin-down electrons to the opposite film edges. One of the authors calculated the AH conductance for a spin current in the presence of SOS.<sup>10</sup> It can be expressed by an anomalous Hall cross section  $a_{xy}$ . (We use the symbol  $a$  for the cross section instead of  $\sigma$  to avoid confusion with the conductivity  $\sigma$ .) If we restrict ourselves to  $(s, p)$ -scattering then the dominant term of the cross section  $a_{xy}$  is

$$a_{xy} \approx -\frac{4\pi}{3k_F^2} \sin(\delta_{1,+} - \delta_{1,-}) \sin \delta_0 \cos(\delta_{1,+} + \delta_{1,-} - \delta_0). \quad (\text{A1})$$

(The full, lengthy expression for  $a_{xy}$  is given in Ref. 10.) Here  $k_F$  is the Fermi wave vector and  $\delta_{l,\pm}=\delta_{l\pm 1/2,l}$  are the Friedel phase shifts for spin-up and spin-down electrons with the orbital and total angular momenta  $l$  and  $j=l\pm 1/2$ . The physical meaning of this cross section is the following: A current density  $j_{x,\uparrow}$  of spin-up electrons ( $\uparrow\parallel\hat{z}$ ) encounters a SOS impurity. Due to the asymmetric SOS a fraction of the current is deflected in the  $y$  direction. This fraction is a current  $I_{y,\uparrow}$  which is equal to the current density times the cross section  $a_{xy}$ :  $I_{y,\uparrow}=a_{xy}j_{x,\uparrow}$ . This current decays after the time  $\tau_0$ , i.e., after the distance of the MFP  $l_0$ . For a SOS impurity concentration  $n_i$  one obtains an AH current density in the  $y$  direction of

$$j_{y,\uparrow} = l_0 n_i a_{xy} j_{x,\uparrow}.$$

For the spin-down electrons one obtains an AH current density with the opposite sign

$$j_{y,\downarrow} = -l_0 n_i a_{xy} j_{x,\downarrow}.$$

So the total current density in the y direction is

$$j_y = l_0 n_i a_{xy} (j_{x,\uparrow} - j_{x,\downarrow}) = p l_0 n_i a_{xy} j_c = p n_i a_{xy} \frac{ne^2}{\hbar k_F} l_0^2 E_x,$$

where  $p = (j_{x,\uparrow} - j_{x,\downarrow}) / (j_{x,\uparrow} + j_{x,\downarrow})$  is the polarization of the current density. The resulting (spin Hall) conductivity is

$$\sigma_{xy} = p n_i a_{xy} \frac{ne^2}{\hbar k_F} l_0^2. \quad (\text{A2})$$

The resulting AH angle is  $\tan \alpha = j_y / j_x = p l_0 n_i a_{xy}$ . The AH angle, the MFP, and the impurity density are experimentally known. The AH cross section  $a_{xy}$  is known in terms of the Friedel phase shifts. If someone would calculate the Friedel phase shifts  $\delta_{l_{\pm 1/2,l}}$  one could directly measure the polarization of the current by means of the AH conductance.

### b. Inhomogeneous spin current

In our experiment the FeCs interface acts as the source of spin current. The appropriate treatment would be using the Boltzmann equation. If one includes the size effect in the thin films then the problem becomes rather involved. We treat the problem here in a simplified fashion. We divide the charge current density  $j_c(z)$  in the Cs film into  $[j^+(z) + j^-(z)]$ . The superscript gives the sign of the  $k_z$  component of the involved electrons. Here  $j_c^-(z) = [j_{\uparrow}^-(z) + j_{\downarrow}^-(z)]$  is the part of the charge current with  $k_z < 0$  which moves towards the interface. Similarly  $j_c^+(z) = [j_{\uparrow}^+(z) - j_{\downarrow}^+(z)]$  is the (part of the) spin current with  $k_z > 0$  which moves away from the surface. To keep the derivation simple we assume that the spin current is small compared with the charge current, i.e.,  $[[j_{\uparrow}^+(z) - j_{\downarrow}^+(z)]] \ll [j_{\uparrow}^+(z) + j_{\downarrow}^+(z)]$  and that the charge current with positive and negative  $k_z$  are similar  $|j^+(z) - j^-(z)| \ll [j^+(z) + j^-(z)]$ .

At the FeCs interface the spin-up and spin-down electrons experience a different degree of specular reflection,  $\lambda_{\uparrow}$  and  $\lambda_{\downarrow}$ . The specular part of the reflected electrons maintains the accumulated drift velocity and contributes a current density  $j^+(0) = \lambda_{\uparrow} j_{\uparrow}^+(0) + \lambda_{\downarrow} j_{\downarrow}^+(0)$  at  $z=0$ . When  $\lambda_{\uparrow} \neq \lambda_{\downarrow}$  then the interface generates a spin current  $j_s^+$  which moves away from the interface into the Cs and is given (in first approximation) by  $j_s^+(0) = \lambda j_c^-(0)$  where  $\lambda = \lambda_{\uparrow} - \lambda_{\downarrow}$ . From now on the electric field has no effect on the size of the spin current.

The electrons (of the spin current) with  $k_z > 0$  move with an average velocity  $\alpha v_F$  away from the interface into the Cs. Here  $v_F$  is the Fermi velocity and  $\alpha$  is of the order of 1/2. Within the Cs film both electron spins experience the same relaxation time  $\tau_0$ . Therefore  $\tau_0$  is the decay time for both the charge current and the spin current, for example,  $dj_s^+/dt = -j_s^+/\tau_0$ . In the stationary situation this yields a spatial decay of the spin current.

$$\frac{\partial j_s^+}{\partial z} = \frac{dj_s^+}{dt} \bigg/ \frac{dz}{dt} = -\frac{1}{\tau_0} \frac{1}{\alpha v_F} j_s^+$$

which yields

$$\begin{aligned} j_s^+(z) &= j_s^+(0) \exp\left(-\frac{z}{\alpha v_F \tau_0}\right) = j_s^+(0) \exp\left(-\frac{z}{l_{chr}}\right) \\ &= \lambda j_c^-(0) \exp\left(-\frac{z}{l_{chr}}\right) = \frac{\lambda}{2} j_c(0) \exp\left(-\frac{z}{l_{chr}}\right). \end{aligned} \quad (\text{A3})$$

If there is a finite specular reflection  $r$  at the upper surface then part of the spin current  $j_s^+$  is reflected at the upper surface. This results in a spin current which propagates in the negative  $z$  direction and has the form

$$j_s^-(z) = j_s^-(d_{Cs}) \exp\left(-\frac{d_{Cs} - z}{l_{chr}}\right) = \frac{r\lambda}{2} j_c(0) \exp\left(-\frac{2d_{Cs} - z}{l_{chr}}\right).$$

In the following we neglect the specular reflection at the upper surface and we treat the charge current density as constant in the film. Then the polarization  $p(z)$  of the current density is position dependent.

$$p(z) = \frac{j_{\uparrow}(z) - j_{\downarrow}(z)}{j_{\uparrow}(z) + j_{\downarrow}(z)} = \frac{\lambda}{2} \exp\left(-\frac{z}{l_{chr}}\right).$$

To obtain the total AH conductance  $L_{xy}$  one has to integrate Eq. (A2) over  $dz$ .

$$\begin{aligned} L_{xy} &= n_i a_{xy} \frac{ne^2}{\hbar k_F} l_0^2 \int_0^d p(z) dz \\ &= \frac{1}{2} \lambda n_i a_{xy} \frac{ne^2}{\hbar k_F} l_0^2 l_{chr} \left[1 - \exp\left(-\frac{d_{Cs}}{l_{chr}}\right)\right]. \end{aligned} \quad (\text{A4})$$

Our experimental results agree within the accuracy of the measurement with the contribution of Eq. (A4).

## 4. Interface localization

Our group recently investigated the effect of surface impurities on the conductance of alkali films using the superconducting proximity effect.<sup>22</sup> In these experiments it was demonstrated that the conductance of a 5 nm thick K film on top of a Pb film lost its conductance when covered with a submonolayer of Pb; but it maintained its full ability to reduce the superconducting transition temperature of the Pb film. As discussed in Ref. 22 this is the behavior of localized electrons in the K whose localization length is larger than the film thickness. Then electrons in the layer can move perpendicular but not parallel to the layer.

Such a surface localization would explain why the AHE of Pb or Au impurities on top of an FeCs double layer disappears when the impurity coverage exceeds 0.03 atomic layer. The conductance and AHC plot in Fig. 2 and Figs. 5 and 6 suggest that the Au coverage repeatedly introduces surface localization or its precursor for the Cs conduction electrons. The condensation of the next Cs layer essentially removes this localization so that the Au impurities contribute to the AHC. It is also likely that the MFP of the conduction

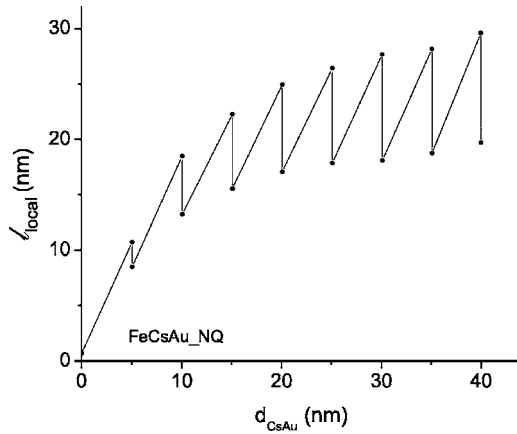


FIG. 7. The local mean free path in the  $\text{Fe}(\text{CsAu})_\nu$  multilayer derived from the experiment.

electrons in the  $(\text{CsAu})_\nu$  layers is anisotropic. The perpendicular MFP will be larger than the parallel one.

### 5. Local mean free path

In Fig. 3 the average MFP of the conduction electrons in Cs with Au or Ag impurities is plotted. In this evaluation the conductance of the whole Cs film divided by the total Cs is evaluated. The MFP is calculated from the resulting conductivity. This evaluation is appropriate for pure films. The structure of their initial layer recrystallizes somewhat when the initial layer is covered with the same material. When, however, the individual Cs layers are separated by a thin Au or Ag submonolayer then the structure of the previous layers can be frozen. In this case a local MFP might be more appropriate. It is calculated from the local conductivity  $\Delta L_{xx}/5 \text{ nm}$ .  $\Delta L_{xx}$  is the conductance of the multilayer minus the conductance of the last  $\text{Fe}(\text{CsAu})_\nu$ . For the upper points in Fig. 7 one has  $\Delta L_{xx} = L_{xx}[\text{Fe}(\text{CsAu})_\nu \text{Cs}] - L_{xx}[\text{Fe}(\text{CsAu})_\nu]$  and for the lower points  $\Delta L_{xx} = L_{xx}[\text{Fe}(\text{CsAu})_{\nu+1}] - L_{xx}[\text{Fe}(\text{CsAu})_\nu]$ .

### 6. The normal Hall effect in $\text{Fe}(\text{CsAu})_\nu$ multilayers

The measurement of the Hall effect of the multilayers also yields the Hall constant. Figure 8 shows the local Hall constant as a function of the Cs thickness. The upper points represent the last Cs minilayer and the lower points the last Cs layer with Au coverage. While the Hall constant of the individual Cs layers lies in the range of  $-(63 \pm 3) \times 10^{-11} \text{ m}^3/\text{As}$  as the condensation of the noble metal increases the value to  $-(77 \pm 2) \times 10^{-11} \text{ m}^3/\text{As}$ . The condensation of the Au or Ag impurities acts as if 25% of the Cs layer do no longer contribute to the normal Hall effect.

### 7. Asymmetric Hall curve

In Fig. 9 the Hall curves for  $\text{Fe}(\text{CsAu})_4$  and  $\text{Fe}(\text{CsAg})_4$  are plotted as a function of the magnetic field. The normal Hall conductance is subtracted, but the curves are not symmetrized. It is very obvious that the Hall curve for

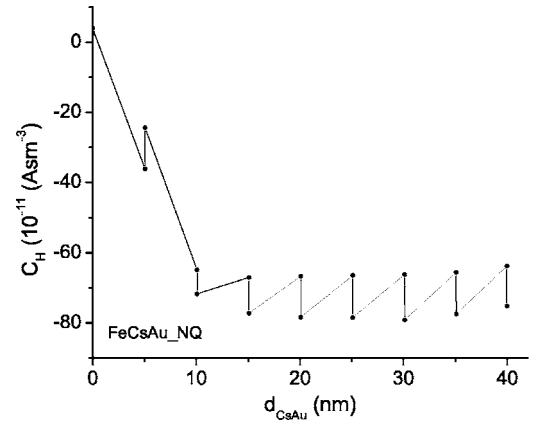


FIG. 8. The experimental local Hall constant for the  $\text{Fe}(\text{CsAu})_\nu$  multilayers as function of the total Cs thickness.

$\text{Fe}(\text{CsAu})_4$  is not antisymmetric. Such a behavior can be easily observed in the magnetoresistance of a ferromagnetic film or multilayer. It occurs when the magnetic field is aligned perfectly perpendicular to the film. If the magnetic field is lowered and approaches  $B=0$  then the magnetic domains align parallel to the film plane. The orientation within the film plane is arbitrary. Therefore the angle between the current and the magnetization of the single domain will be arbitrary too. Generally the resistance is anisotropic and depends on the angle between current and magnetization. Then the resistance at zero and small fields depends on the accidental orientation of the magnetic domains within the film plane. One observes hysteresis. This can be avoided by slightly tilting the film substrate so that the magnetic field is no longer perfectly perpendicular to the film.

On the other hand such hysteresis is generally not observed for the AHE. Only the  $z$  component of the magnetization  $M$  contributes to the AHE. The  $z$  component of the magnetization,  $M_z$ , is equal to the applied magnetic flux  $B$  (for  $B < M$ ). This is demonstrated by the perfectly antisymmetric shape of the AH curve of  $\text{Fe}(\text{CsAg})_4$ . Therefore we

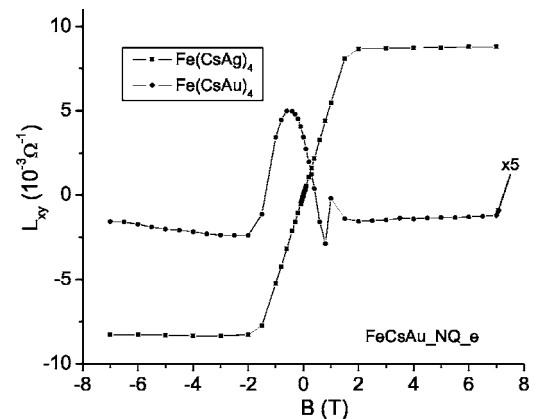


FIG. 9. The experimental anomalous Hall curves for  $\text{Fe}(\text{CsAu})_4$  and  $\text{Fe}(\text{CsAg})_4$  as a function of the magnetic field. The normal Hall effect is subtracted but the curves are not symmetrized.

believe that the asymmetric shape of the AH curve for  $\text{Fe}(\text{CsAu})_4$  contains interesting information about the system. It might suggest that the orientation of the electron spins in this field range is not parallel to the magnetic field. So

far we have not investigated further this observation. It does not effect any of our conclusions because we only used the AHC for the large fields and extrapolated the linear part back to zero.

---

\*Electronic address: bergmann@usc.edu

<sup>1</sup>E. H. Hall, *Philos. Mag.* **12**, 157 (1881).

<sup>2</sup>J. Smit, *Physica (Utrecht)* **16**, 612 (1951).

<sup>3</sup>R. Karpulus and J. M. Luttinger, *Phys. Rev.* **95**, 1154 (1954).

<sup>4</sup>A. Fert and O. Jaoul, *Phys. Rev. Lett.* **28**, 303 (1972).

<sup>5</sup>L. Berger, *Phys. Rev. B* **2**, 4559 (1970).

<sup>6</sup>Y. Yao, L. Kleinman, A. H. MacDonald, J. Sinova, T. Jungwirth, D. S. Wang, E. Wang, and Q. Niu, *Phys. Rev. Lett.* **92**, 037204 (2004).

<sup>7</sup>J. E. Hirsch, *Phys. Rev. Lett.* **83**, 1834 (1999).

<sup>8</sup>L. E. Ballentine and M. Huberman, *J. Phys. C* **10**, 4991 (1977).

<sup>9</sup>M. Huberman and L. E. Ballentine, *Can. J. Phys.* **56**, 704 (1978).

<sup>10</sup>G. Bergmann, *Phys. Rev. B* **63**, 193101 (2001).

<sup>11</sup>M. I. Dyakonov and V. I. Perel, *Phys. Lett.* **35A**, 459 (1971).

<sup>12</sup>W.-K. Tse, J. Fabian, I. Zutic, and S. Das Sarma, *Phys. Rev. B* **72**, 241303(R) (2005).

<sup>13</sup>V. Sih, R. C. Myers, Y. K. Kato, W. H. Lau, A. C. Gossard, and

D. D. Awschalom, *Nature Phys.* **1**, 31 (2005).

<sup>14</sup>J. Wunderlich, B. Kaestner, J. Sinova, and T. Jungwirth, *Phys. Rev. Lett.* **94**, 047204 (2005).

<sup>15</sup>I. Zutic, J. Fabian, and S. Das Sarma, *Rev. Mod. Phys.* **76**, 323 (2004).

<sup>16</sup>J. P. Bird and Y. Ochiai, *Science* **303**, 1621 (2004).

<sup>17</sup>S. A. Wolf, D. D. Awschalom, R. A. Buhrman, J. M. Daughton, S. v. Molnár, M. L. Roukes, A. Y. Chtchelkanova, and D. M. Treger, *Science* **294**, 1488 (2001).

<sup>18</sup>D. D. Awschalom, M. E. Flatte, and N. Samarth, *Sci. Am.* **286**, 66 (2002).

<sup>19</sup>G. Bergmann, F. Song, and D. Garrett, *Phys. Rev. B* **70**, 020404 (2004).

<sup>20</sup>G. Bergmann, *Phys. Rev. Lett.* **41**, 1619 (1978).

<sup>21</sup>G. Bergmann, *Phys. Rev. B* **19**, 3933 (1979).

<sup>22</sup>M. Zhang and G. Bergmann, *Europhys. Lett.* **69**, 442 (2005).